

# Optical tweezers-based probe of charge transfer in organic semiconductors at microscopic scales

Rebecca R. Grollman, Jacob Busche, and Oksana Ostroverkhova

Department of Physics, Oregon State University, Corvallis, OR 97331

## ABSTRACT

We present a technique to study the (dis)charging of organic semiconductor films at microscopic scales, and in various environments, using an optical tweezers-based method combined with fluorescence spectroscopy. The  $1\ \mu\text{m}$  silica spheres were coated with either pristine organic semiconductor or a donor-acceptor blend, trapped using optical tweezers, and their fluorescence was measured concurrently with the effective surface charge. The effective surface charge in uncoated silica spheres suspended in water was a factor of  $\sim 70$  higher as compared to that from similar spheres in a nonpolar toluene. In contrast, the coated silica spheres exhibited low effective charge densities in both environments, which is indicative of minimal interaction of organic semiconductors under study with these environments. This serves as a proof-of-principle experiment towards systematic studies of nanoscale photoinduced charge-based interactions between organic semiconductor molecules, with a resolution down to an elementary charge, and depending on the dielectric environment.

**Keywords:** Optical tweezers, effective charge, organic semiconductors, charging dynamics

## 1. INTRODUCTION

Organic semiconductors have attracted attention due to their low cost, easy fabrication, and tunable properties. Applications of organic semiconductors include light-emitting diodes, solar cells, thin-film transistors (TFTs), and many others.<sup>1</sup> Most of these applications rely on the material's conductive or photoconductive properties, and therefore it is important to understand processes of charge carrier generation and charge transfer, which are mediated by dielectric properties of local nanoenvironment. Our goal is to develop a non-contact optical tweezers-based method to measure charge carrier generation and charge transfer in organic semiconductors, at nanoscales, with an elementary charge resolution, and in systematically varied environments. Optical tweezers have been utilized in many applications including biology, chemistry, engineering, and physics.<sup>2</sup> Optical tweezers use a highly focused laser beam to optically trap micron-sized particles. By applying an AC electric field to an optically trapped particle, measurement of the surface charge of  $1\ \mu\text{m}$  PMMA sphere suspended in dodecane with single charge resolution was demonstrated.<sup>3</sup> Recently, it has also been shown that it is possible to measure the (dis)charging dynamics of a similar system using high electric fields and high sampling rates.<sup>4</sup> In this paper, we report on the development of an optical tweezers system which enables measurements of the photoinduced (dis)charging dynamics of spheres coated with organic semiconductors and their donor-acceptor (D/A) blends, in polar and nonpolar environments.

## 2. MATERIALS AND METHODS

### 2.1 Materials

For our studies, we chose a fluorinated anthradithiophene (ADT) derivative functionalized with (triethylsilyl)ethynyl (TES) side groups, ADT-TES-F, a cyano-substituted ADT derivative functionalized with (triisopropylsilyl)ethynyl (TIPS) side groups, ADT-TIPS-CN (Fig. 1), and a fluorinated pentacene (Pn) derivative functionalized with TIPS groups (Pn-TIPS-F8, Fig. 1). The ADT-TES-F derivative has shown TFT charge carrier (hole) mobilities of over  $1.5\ \text{cm}^2/(\text{Vs})$ ,<sup>5</sup> fast charge carrier photogeneration,<sup>6,7</sup> and high photoconductivity under continuous wave (cw) illumination.<sup>8</sup> The ADT-TIPS-CN and Pn-TIPS-F8 derivatives have been used as acceptors in donor-acceptor (D/A) bulk heterojunctions (BHJs) with polymer or ADT-TES-F donors.<sup>9-14</sup> The ADT-TES-F/ADT-TIPS-CN and ADT-TES-F/Pn-TIPS-F8 blends exhibit strong exciplex formation with the peak energy corresponding to HOMO(D)-LUMO(A), which yields 1.86 eV ( $\sim 669\ \text{nm}$ ) and 1.72 eV ( $\sim 723\ \text{nm}$ ), respectively.<sup>11,13</sup>

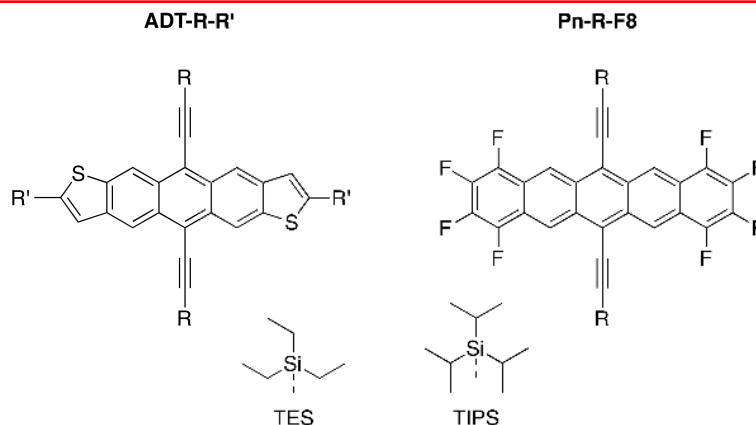


Figure 1. Molecular structures of ADT-R-R' and Pn-R-F8 with TES and TIPS side groups (R). End groups (R') for ADT-R-R' could be either F or CN.

## 2.2 Sample Preparation

Amorphous silica spheres 1  $\mu\text{m}$  in diameter (Thermo Scientific,  $0.99 \pm 0.02 \mu\text{m}$ , refractive index  $n = 1.40 - 1.46$ , 2% suspension in water) were coated with ADT-TES-F or Pn-TIPS-F8 molecules as follows. A 2  $\mu\text{L}$  solution of silica spheres in water was added to 50  $\mu\text{L}$  30 mM stock solution of ADT-TES-F or Pn-TIPS-F8 in toluene and sonicated for 20 minutes. Then, 14  $\mu\text{L}$  of the mixture was added to 4 mL of ultra-pure millipore (Milli-Q, 18  $M\Omega$  cm) water, sonicated for 5 minutes, and left unperturbed overnight. As control samples, we used uncoated silica spheres, also suspended in water. Additionally, we prepared solutions of ADT-TES-F-coated silica spheres and uncoated silica spheres in toluene following the same procedure, but replacing water with toluene at the last step of the procedure. Finally, we prepared spheres coated with an ADT-TES-F (donor) and ADT-TIPS-CN (acceptor) D/A blend. A 30 mM stock solution of ADT-TES-F in toluene and 2 mM stock solution of ADT-TIPS-CN in toluene were sonicated for 10 minutes. 2 mL of the ADT-TES-F stock solution and 526  $\mu\text{L}$  of the ADT-TIPS-CN stock solution were combined and sonicated for 10 minutes. Next, 4  $\mu\text{L}$  solution of silica spheres in water was added to 100  $\mu\text{L}$  the ADT-TES-F and ADT-TIPS-CN solution and sonicated for 20 minutes. Lastly, 14  $\mu\text{L}$  of the silica and D/A solution was added to 4 mL of millipore water, sonicated for 5 minutes, and left unperturbed overnight. We chose millipore water and toluene for our initial set of experiments because they did not compromise the quality of the coating and because they provided environments with considerably different dielectric permittivity ( $\epsilon = 80$  and 2.38, respectively). The ADT-TES-F and ADT-TES-F/ADT-TIPS-CN (Pn-TIPS-F8) coatings were confirmed using fluorescence microscopy at 532 nm (633 nm) cw excitation, which resulted in strong emission by the coatings at wavelengths of  $>580$  nm ( $>650$  nm)<sup>8</sup> as shown in Fig. 2. No fluorescence was observed from uncoated silica spheres.

Once solutions of coated spheres were prepared, they were inserted into a sample holder with coplanar electrodes as shown in the inset of Fig. 2. Details on sample holder preparation can be found elsewhere.<sup>15</sup> Spheres were trapped in the center of the electrode gap to minimize edge effects. Spheres were trapped at a depth of about 20  $\mu\text{m}$  away from the top of the coverslip to avoid interactions between the sphere and glass slide.

## 2.3 Optical Tweezer Trapping Setup

Optical tweezer trapping was performed in a custom inverted microscope assembly with an oil immersion microscope objective (Edmund Optics, 100X, NA of 1.25, 160 mm tube length) as shown in Fig. 2.<sup>16</sup> Spheres were trapped with a cw 800 nm Ti:Sapphire laser (KM Labs, Inc.). For uncoated silica spheres and silica spheres coated with ADT-TES-F or ADT-TES-F/ADT-TIPS-CN D/A blend (silica spheres coated with Pn-TIPS-F8), the position of the trapped sphere was detected by the scattering of a cw 633 nm Helium-Neon laser (cw 532 nm laser, Verdi V5, Coherent, Inc.) detected by a Hamamatsu S4349 quadrant photodiode (QPD). The QPD signal was collected using a data acquisition card (DAQ) (NI-6221) read out by a custom LabVIEW program.

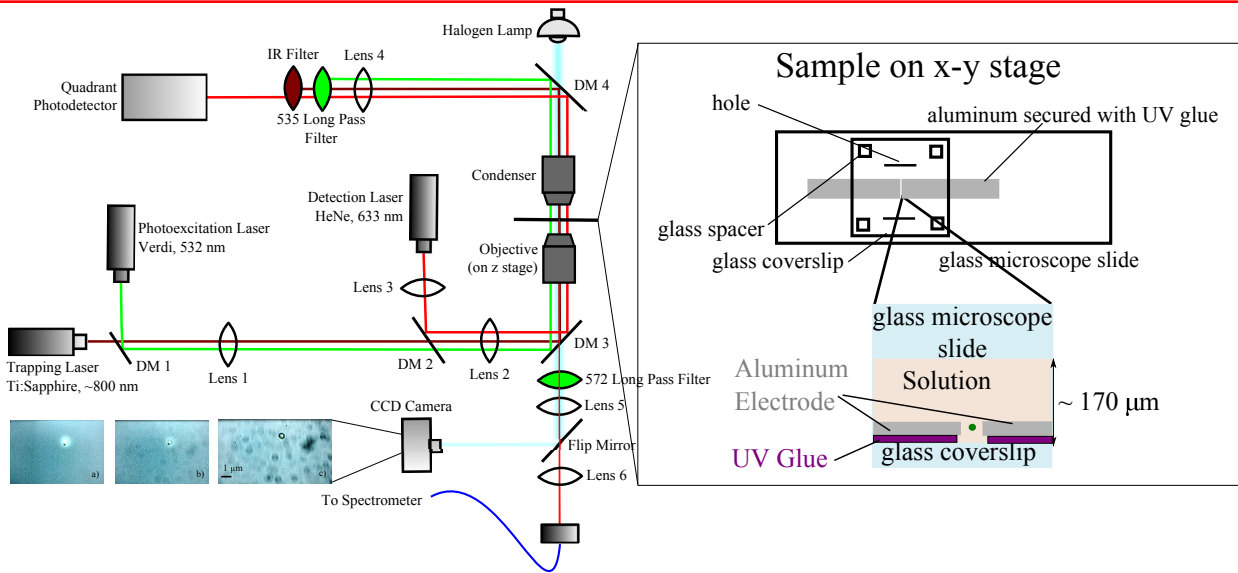


Figure 2. The experimental set up used to measure effective charge, which includes an 800 nm trapping laser, 633 nm (532 nm) detection laser, and 532 nm (633 nm) photoexcitation laser for the ADT-TES-F-coated (Pn-TIPS-F8-coated) spheres. The images are of a trapped ADT-TES-F coated silica sphere: (a) under 532 nm excitation (halogen lamp off), (b) under 532 nm excitation (halogen lamp on), and (c) no excitation (halogen lamp on). Fluorescence emission of the ADT-TES-F coating can be seen in (a) and (b). The sample holder design is shown on the right.

Additionally, a cw 532 nm (633 nm) laser beam, collimated to minimize its effect on the trap stability, was used to photoexcite ADT-TES-F (Pn-TIPS-F8) in ADT-TES-F-coated or ADT-TES-F/ADT-TIPS-CN-coated spheres (Pn-TIPS-F8-coated spheres). Spheres were imaged with a CCD camera and halogen lamp. When assessing fluorescence from an ADT-TES-F coating, a long-pass 572 nm filter was placed in front of the CCD camera to transmit the fluorescence emission of the ADT-TES-F molecules, while blocking the 532 nm excitation. Filters were also placed in front of the QPD to block the 800 nm and 532 nm light. For spheres with a Pn-TIPS-F8 coating, a 632.8 nm notch filter was placed in front of the CCD camera to block light from the 633 nm excitation laser. A band pass filter was placed in front of the QPD to block emission from the spheres, but allow the scattering of the 532 nm light to pass. An IR filter was also placed in front of the QPD to block the trapping laser.

## 2.4 Trap stiffness and charge measurements

The trap stiffness  $k$  of a trapped sphere is a defining characteristic that can be used to monitor the stability of the optical tweezers trap as well as determine the surface charge on a trapped sphere when an AC electric field is applied. The trap stiffness in the x-y plane was calculated by applying four analysis methods to the data including applying the equipartition theorem to the variance of the sphere's motion in the trap, performing a Gaussian fit to a histogram of the sphere's position in the trap, obtaining the corner frequency in the power spectrum of the suppressed Brownian motion of the sphere, and fitting the data with the parabolic function describing the potential well.<sup>16</sup> The power spectrum of the position fluctuations is given by

$$|\tilde{x}(f)^2| = \frac{k_B T}{\pi^2 \beta (f_c^2 + f^2)}, \quad (1)$$

where  $f$  is the frequency,  $\beta$  is the drag coefficient of the sphere in the medium, and  $f_c$  is the corner frequency. In particular, the corner frequency is related to the trap stiffness as  $f_c = k/(2\pi\beta)$ ,<sup>16</sup> from which the trap stiffness is readily obtained.

When an AC electric field is applied to the trapped sphere, another component is added to the power spectrum such that it becomes

$$|\tilde{x}(f)^2| = \frac{k_B T}{\pi^2 \beta (f_c^2 + f^2)} + \frac{k_B T \gamma^2}{2k} [\delta(f - f_{AC})], \quad (2)$$

where  $\gamma^2$  is the scaled ratio of the mean square periodic and Brownian forces and can be calculated from

$$P_{AC} = \int_{-\infty}^{\infty} |\tilde{x}(f)^2|_E df = \frac{k_B T}{k} \gamma^2, \quad (3)$$

where  $|\tilde{x}(f)^2|_E$  is the power spectrum due to the applied electric field.<sup>3</sup> As shown in Ref. 3 the effective charge  $Z_{eff}$  on a sphere can be calculated with

$$e|Z_{eff}| = \frac{\gamma \beta}{E} \sqrt{\frac{2k_B T}{k} ((2\pi f_{AC})^2 + (k/\beta))}, \quad (4)$$

where  $e$  is the charge of an electron,  $E$  is the applied electric field, and  $f_{AC}$  is the driving frequency of the electric field.

To measure the effective charge of our spheres, we applied an AC voltage of 2.5  $V_{pp}$  to 20  $V_{pp}$  across our electrodes using an amplified sinusoidal signal from a function generator (Tektronix AFG3021). Frequencies  $f_{AC}$  ranging from 30 Hz to 500 Hz were tested, and charge measurements at frequencies in the range between 70 and 110 Hz yielded most consistent data, prompting us to select a driving frequency of 70 or 110 Hz for most experiments reported here. The electric field was estimated as  $\lambda \frac{V}{d}$  where  $V$  is the applied voltage and  $d$  is the distance between electrodes. The scaling factor  $\lambda$ , described in Ref. 3, takes into account the electric field dependence on the position of the sphere with respect to the electrodes. In order to probe changes in effective charge density upon photoexcitation of ADT-TES-F in ADT-TES-F-coated spheres, we performed charge measurements under 532 nm excitation at powers of up to 28 mW.

### 3. RESULTS AND DISCUSSION

In order to confirm coating of the silica spheres, we obtained fluorescence spectra of the coating of trapped spheres in water under a 532 nm or 633 nm excitation, depending on the coating. Fig. 3 demonstrates the fluorescence of a silica sphere coated with ADT-TES-F and of a sphere coated with the ADT-TES-F/ADT-TIPS-CN D/A blend. The ADT-TES-F-coated spheres exhibited fluorescence emission with a maximum at  $\sim 590$  nm, consistent with that from pristine ADT-TES-F films previously studied in thin-film devices.<sup>10,17</sup> The fluorescence emission from the ADT-TES-F/ADT-TIPS-CN D/A blend coating was dominated by that from the ADT-TES-F/ADT-TIPS-CN exciplex at  $\sim 669$  nm, also consistent with that from the ADT-TES-F/ADT-TIPS-CN films.<sup>13</sup> While in our present studies the fluorescence emission is used to confirm quality of our coatings, quantitative analysis of fluorescence as a function of applied electric field can be used to monitor exciton (in pristine materials) or exciplex (in D/A blends) dissociation into charge carriers. This can be then combined with monitoring of the total effective charge on the organic semiconductor coating (described below), to quantify photoexcited charge exchange between the organic semiconductor molecules in the coating and in the surrounding environment (e.g. organic acceptors introduced in the surrounding solvent).

Charge measurements were performed by tracking the position of a trapped sphere with an applied AC electric field. Fig. 4 shows two of the methods for calculating trap stiffness, which also demonstrates the presence of charge on the sphere. The histograms (Fig. 4a) are used to calculate trap stiffness without an electric field. In the presence of an electric field, the histogram broadens, with the broadening increasing as the electric field increases. The alternating electric field makes it possible for the sphere to spend more time away from the center of the trap since there is now an electric force in addition to Brownian motion. The addition of the electric force also decreases trap stiffness  $k$ . The power spectral density (PSD) (Fig. 4b) also demonstrates the presence of charge on the sphere, as there is a response at the 110 Hz driving frequency of the AC electric field, which increases as the electric field increases. Silica spheres in water exhibited a much larger response to the AC electric field, as compared to those in toluene. In particular, in water the AC field-driven sphere oscillations overriding the

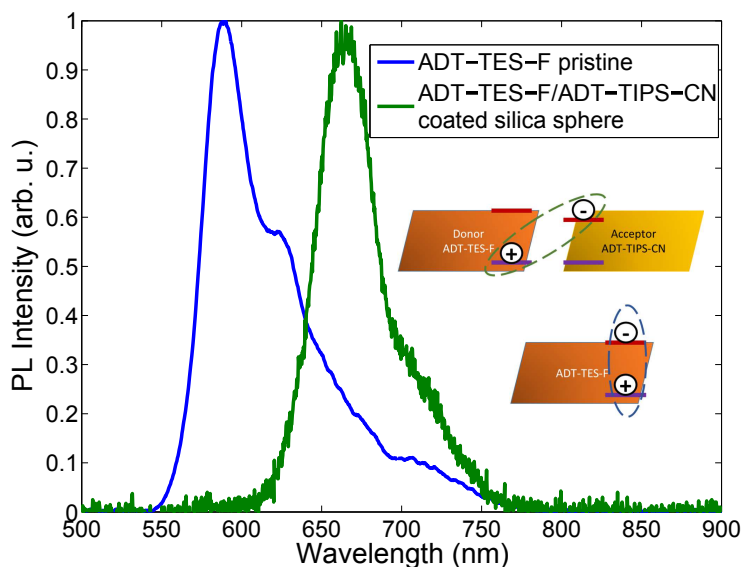


Figure 3. Fluorescence from an ADT-TES-F-coated silica sphere and an ADT-TES-F/ADT-TIPS-CN (D/A blend)-coated silica sphere. Fluorescence emission from the D/A coated sphere is due to the exciplex formed between the donor and acceptor molecules. Inset shows schematics of the emissive ADT-TES-F exciton and of the ADT-TES-F/ADT-TIPS-CN exciplex.

suppressed Brownian motion of a trapped sphere could be observed within our range of applied electric fields.<sup>15</sup> These oscillations were not apparent in toluene, consistent with a considerably smaller charge density on silica spheres in toluene as compared to water (see Table 1). The measured  $P_{AC}$  of Eq. 3 shows a linear relationship with  $E^2$ , in agreement with Eqs. 3 & 4 (Fig. 5) for both environments. A larger slope in the case of uncoated silica spheres in water corresponds to a larger effective charge on the sphere as compared to that on similar spheres in toluene.

The negative charge on the surface of silica spheres in water has been attributed to the dissociation of silanol groups.<sup>18</sup> For example, a surface charge density of  $-700 \pm 150 e/\mu\text{m}^2$  was obtained in Ref. 18, while we obtained  $-290 \pm 95 e/\mu\text{m}^2$ , which represent a very good agreement given that the modifications to the electric field in the vicinity of our spheres have not been taken into account. As shown in Table 1, surface charge decreases by more than an order of magnitude for silica spheres coated with ADT-TES-F or Pn-TIPS-F8 in water. This is consistent with very weak interaction between organic semiconductor molecules of interest, ADT-TES-F and Pn-TIPS-F8, and water. The amount of residual surface charge (Table 1) is similar for ADT-TES-F and Pn-TIPS-F8 coatings could be due to a non-uniform coverage of the sphere by organic semiconductor molecules, which would enable residual interaction of the silica with water.

Both uncoated and organic semiconductor-coated spheres suspended in nonpolar toluene exhibited a low effective surface charge, which suggests weak or no interaction of either silica or organic semiconductor molecules with toluene. This is consistent with observations of low surface charge on PMMA spheres suspended in (nonpolar) dodecane in similar experiments.<sup>3,4</sup> No degradation of the coatings or changes in the total surface charge density were observed for spheres suspended in toluene over the period of at least 6 hours of experimental observation.

Experiments in addition to the total effective charge measurements, that enable measurements of the (dis)charging dynamics require application of high electric fields.<sup>4</sup> Along these lines, we demonstrated that our experiments described above are possible at high electric fields on the order of 1 MV/m. Finally, the effective surface charge density was also measured under continuous photoexcitation of the optically trapped coated spheres. The total effective surface charge density was comparable to that of similar spheres without photoexcitation. This indicates that there is no exchange of charge carriers photoinduced in the organic semiconductor coating and either water or toluene, as expected in the absence of acceptor molecules in the solvent.

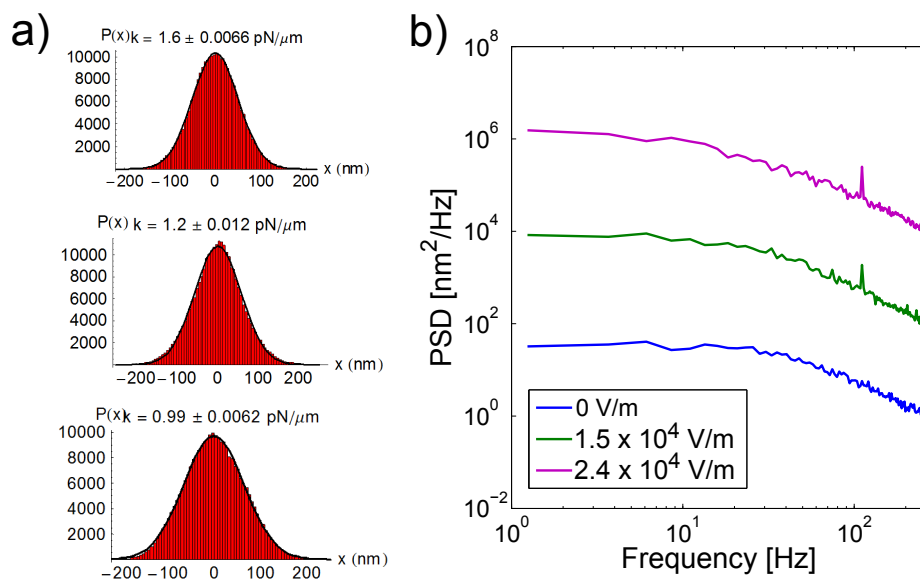


Figure 4. a) Top: No electric field; Middle:  $1.5 \times 10^4$  V/m; Bottom:  $2.4 \times 10^4$  V/m. b) Power spectral densities for silica in toluene with varying applied electric fields. The peak at the driving frequency of 110 Hz increases as the electric field increases.

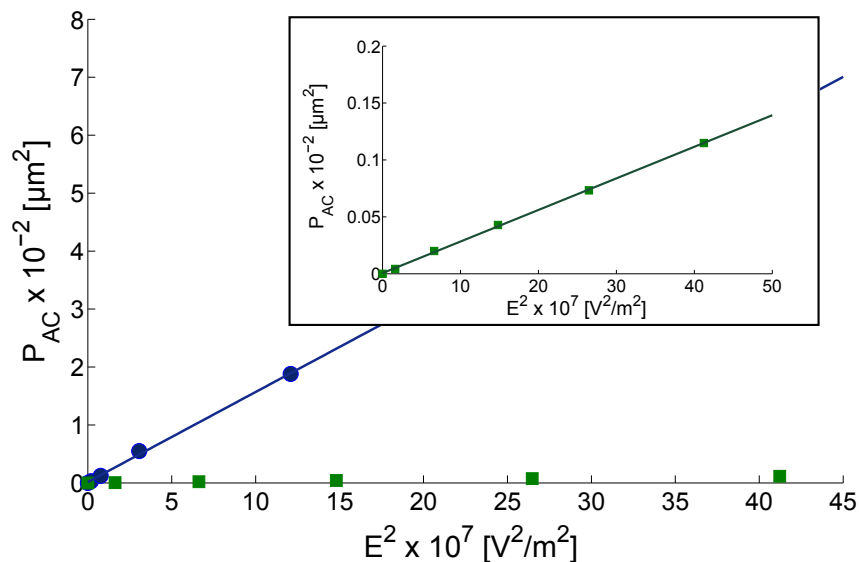


Figure 5. The measured  $P_{AC}$  of Eq. 3 for **Blue circle** : uncoated silica spheres; **Green square** : silica spheres coated with ADT-TES-F. Both types of spheres were suspended in water. Linear fits to Eqs.3 & 4 are also shown. Slopes correspond to the amount of effective charge on sphere.

Our ability to measure effective charge on the organic semiconductor-coated microspheres, concurrently with fluorescence, and in both highly polar and nonpolar environments, lays foundations for systematic studies of photoinduced charge photogeneration and charge transfer, at microscopic scales and potentially with a single charge resolution,<sup>4</sup> as a function of dielectric permittivity of the surrounding environment.

Table 1. Effective surface charge measured for various spheres in water and toluene. The values were averaged over 5-7 spheres of the same type and over at least 9 data runs for each sphere. The error bars reflect sphere-to-sphere variation. The run-to-run error for each given sphere was less than 5%.

Sphere Type	Surface Charge ( $e/\mu m^2$ )	
	Water	Toluene
Silica	$290 \pm 95$	$4 \pm 1$
Silica coated with ADT-TES-F	$13 \pm 5$	$7 \pm 1$
Silica coated with Pn-TIPS-F8	$22 \pm 13$	

#### 4. CONCLUSIONS

We demonstrated the ability to measure the surface charge density of silica microspheres coated with organic semiconductor films in (polar) water and (nonpolar) toluene, concurrently with measurements of fluorescence emission from the coatings, using an optical tweezers-based technique. Organic semiconductor coatings of the microspheres exhibited similar fluorescence properties of those of corresponding films in thin-film devices. The silica spheres coated with the organic semiconductor molecules suspended in water had a surface charge density lower by more than an order of magnitude than uncoated silica spheres, which suggests that the organic semiconductor molecules did not interact with water. Both coated and uncoated spheres suspended in toluene had an even lower surface charge density of below  $10 e/\mu m^2$ , indicative of minimal interactions between either the silica or organic semiconductor molecules with toluene. A non-contact capability to measure effective surface charge in environments with highly varying dielectric permittivity can be utilized in systematic studies of photoinduced charge transfer and exciton and exciplex dissociation in organic semiconductors at microscopic scales.

#### ACKNOWLEDGMENTS

We thank Prof. J. E. Anthony for ADT-TES-F, ADT-TIPS-CN, and Pn-TIPS-F8 and Prof. D. H. McIntyre for providing data analysis software. This work was supported in part by the National Science Foundation grant DMR-1207309.

#### REFERENCES

1. O. Ostroverkhova, ed., *Handbook of organic materials for optical and (opto)electronic devices*, Woodhead Publishing, Cambridge, U.K., 2013.
2. A. Ashkin, "History of optical trapping and manipulation of small-neutral particle, atoms, and molecules," *IEEE J. Sel. Top. Quantum Electron* **6**, pp. 841–856, 2000.
3. G. S. Roberts, T. A. Wood, W. J. Frith, and P. Bartlett, "Direct measurement of the effective charge in nonpolar suspensions by optical tracking of single particles," *J. Chem. Phys.* **126**, p. 194503, 2007.
4. F. Beunis, F. Strubbe, K. Neyts, and D. Petrov, "Beyond millikan: The dynamics of charging events on individual colloidal particles," *Physical Review Letters* **108**, p. 016101, 2012.
5. S. Park, D. A. Mourey, S. Subramanian, J. E. Anthony, and T. N. Jackson, "High-mobility spin-cast organic thin film transistors," *Applied Physics Letters* **93**, p. 043301, 2008.
6. J. Day, A. D. Platt, O. Ostroverkhova, S. Subramanian, and J. Anthony, "Organic semiconductor composites: influence of additives on the transient photocurrent," *Applied Physics Letters* **94**, p. 013306, 2009.

7. J. Day, A. Platt, S. Subramanian, J. Anthony, and O. Ostroverkhova, "Influence of organic semiconductor-metal interfaces on the photoresponse of functionalized anthradithiophene thin films," *Journal of Applied Physics* **105**, p. 103703, 2009.
8. A. D. Platt, J. Day, S. Subramanian, J. E. Anthony, and O. Ostroverkhova, "Optical, fluorescent, and (photo)conductive properties of high-performance functionalized pentacene and anthradithiophene derivatives," *Journal of Physical Chemistry C* **113**, pp. 14006–14014, 2009.
9. K. Paudel, B. Johnson, A. Neunzert, M. Thieme, B. Purushothaman, M. M. Payne, J. E. Anthony, and O. Ostroverkhova, "Small-molecule bulk heterojunctions: Distinguishing between effects of energy offsets and molecular packing on optoelectronic properties," *Journal of Physical Chemistry C* **117**, pp. 24752–24760, 2013.
10. A. D. Platt, M. J. Kendrick, M. Loth, J. E. Anthony, and O. Ostroverkhova, "Temperature dependence of exciton and charge carrier dynamics in organic thin films," *Physical Review B* **84**, p. 235209, 2011.
11. M. J. Kendrick, A. Neunzert, M. M. Payne, B. Purushothaman, B. D. Rose, J. E. Anthony, M. M. Haley, and O. Ostroverkhova, "Formation of the donor-acceptor charge-transfer exciton and its contribution to charge photogeneration and recombination in small-molecule bulk heterojunctions," *Journal of Physical Chemistry C* **116**, pp. 18108–18116, 2012.
12. K. R. Rajesh, K. Paudel, B. Johnson, R. Hallani, J. E. Anthony, and O. Ostroverkhova, "Design of organic ternary blends and small-molecule bulk heterojunctions: photophysical considerations," *Journal of Photonics for Energy* **5**, p. 057208, 2015.
13. W. E. B. Shepherd, A. D. Platt, M. J. Kendrick, M. Loth, J. E. Anthony, and O. Ostroverkhova, "Energy transfer and exciplex formation and their impact on exciton and charge carrier dynamics in organic films," *Journal of Physical Chemistry Letters* **2**, pp. 362–366, 2011.
14. K. Paudel, B. Johnson, M. Thieme, M. Haley, M. M. Payne, J. E. Anthony, and O. Ostroverkhova, "Enhanced charge photogeneration promoted by crystallinity in small-molecule donor-acceptor bulk heterojunctions," *Applied Physics Letters* **105**, p. 043301, 2014.
15. R. Grollman, K. Peters, and O. Ostroverkhova, "Surface charge measurements and (dis)charging dynamics of organic semiconductors in various media using optical tweezers," *Proc. of SPIE* **8983**, p. 89831N, 2014.
16. M. J. Kendrick, D. H. McIntyre, and O. Ostroverkhova, "Wavelength dependence of optical tweezer trapping forces on dye-doped polystyrene microspheres," *J. Opt. Soc. Am. B* **26**, pp. 2189–2198, 2009.
17. W. E. B. Shepherd, A. D. Platt, D. Hofer, O. Ostroverkhova, M. Loth, and J. E. Anthony, "Aggregate formation and its effect on (opto)electronic properties of guest-host organic semiconductors," *Applied Physics Letters* **97**, p. 163303, 2010.
18. S. H. Behrens and D. G. Grier, "The charge of glass and silica surfaces," *Journal of Chemical Physics* **115**, pp. 6716–6721, 2001.